

**MOLECULAR CONSTITUENTS OF THE MOSS (CO3.6) CHONDRITE VIA MICRO-RAMAN SPECTROSCOPIC IMAGING.** M. Yesiltas<sup>1</sup>, T. D. Glotch<sup>1</sup>, and D. S. Ebel<sup>2</sup>. <sup>1</sup>Department of Geosciences, Stony Brook University 255 ESS Building, Stony Brook, NY 11794-2100. <sup>2</sup>Department of Earth and Planetary Sciences, American Museum of Natural History, New York, NY 10024. [mehmet.yesiltas@stonybrook.edu](mailto:mehmet.yesiltas@stonybrook.edu)

**Introduction:** The Moss chondritic meteorite fell 14 July 2006 in Ostfold, Norway after a bright fireball followed by a loud explosion [1]. Based on initial studies, it is classified as a type 3.6 CO chondrite [1]. According to previous studies, Moss contains small but abundant chondrules and a dark matrix [2] with olivine, troilite, and kamacite embedded in the matrix [1], with an unusually low matrix-to-chondrule ratio [2]. Carbonaceous chondrites contain up to 5.4 wt% carbon, some of which is organic [3]. In Moss, organic matter amounts to a total of ~0.21-0.25 wt% [2], lower than other carbonaceous chondrites [3, 4]. Nevertheless, some organic molecules (e.g., naphthalene), and the mineral graphite are found in Moss [2, 4].

Lower organic content seen in the Moss meteorite suggests a higher degree of thermal metamorphism than that of other members of the CO group [4]; however, since all CO3 chondrites are thought to originate from a single asteroid [2], organic matter seen in the Moss meteorite is not consistent with its thermal metamorphic grade [5]. The type and distribution of molecular compounds present in the Moss meteorite can provide clues to its complex parent body histories. For this purpose, we used confocal micro-Raman spectroscopy and imaging to study the Moss meteorite with high spatial resolution. Here, we identify various organic and inorganic materials present in the samples, and shed light on the processes that the parent body of the Moss meteorite may have been subjected to.

**Sample:** The Moss meteorite studied here was loaned from the American Museum of Natural History in the form of a polished thin section. After receipt, the sample was kept in a desiccator, and taken out prior to measurements. The sample was kept away from any adhesive and outgassing materials in the laboratory in order to minimize terrestrial contamination.

**Method:** Micro-Raman measurements were performed at the Stony Brook University Vibrational Spectroscopy Laboratory using a WiTEC alpha300R confocal Raman imaging system coupled to a 512 nm NdYAG green laser. We used a 50X (NA 0.80) objective, which resulted a spatial resolution of ~0.8  $\mu\text{m}$ . The laser power was 1.3 mW on the sample surface for our experiments, corresponding to a power density level of ~2 mW/ $\mu\text{m}^2$ . After locating a region of interest, we scanned an area of 100  $\mu\text{m}$  X 100  $\mu\text{m}$  with

integration time of 1 second. With such low power density and very short exposure time, there should be no laser-induced damage or heating of the sample.

**Results:** Figure 1 presents a visible reflected light as well as a color-coded overlaid image of the studied region. In the false-color image, blue, yellow, green, and pink colors represent, respectively, carbonaceous matter, pyroxene, olivine, and diamond.

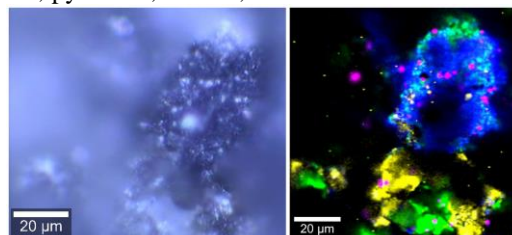


**Figure 1.** Visible reflected light (left), and false-color overlaid (right) images of the studied grain.

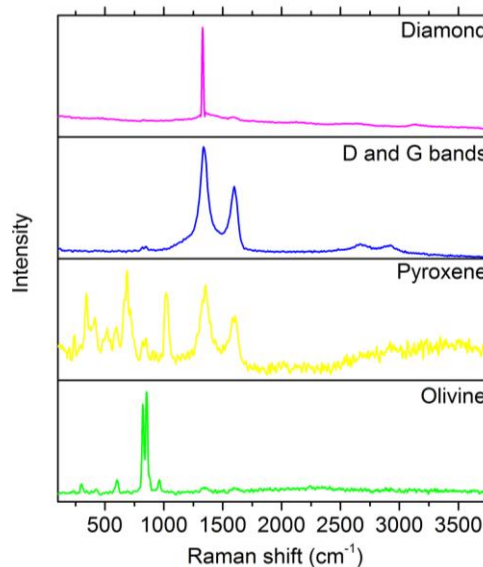


**Figure 2.** Micro-Raman spectra of pixels extracted from the corresponding regions in Figure 1.

We extracted spectra of individual components from the overlaid image shown in Figure 1. Among the observed peaks, those near 1341  $\text{cm}^{-1}$  and 1594  $\text{cm}^{-1}$  are the first order D and G bands due to disordered  $\text{sp}^3$  and graphite-like  $\text{sp}^2$  carbon bonds, respectively. The spectrum of D+G (blue) also presents the second order carbon peaks near 2665  $\text{cm}^{-1}$  and 2920  $\text{cm}^{-1}$ . These carbon peaks suggest that an ordered

state of carbon is present in Moss, unlike the highly disordered state in some primitive chondrites (see Fig.4).

The average spectrum of the pink spots in the overlaid image shows a sharp and strong diamond peak at  $1330\text{ cm}^{-1}$ , and we are currently investigating the source of these diamond particles. The spectrum of olivine (green) presents a doublet feature at  $821\text{ cm}^{-1}$  and  $853\text{ cm}^{-1}$ , indicative of Mg-rich olivine. The two pyroxene bands (yellow) appear at  $688\text{ cm}^{-1}$  and  $1025\text{ cm}^{-1}$ , the spectral profile and shape suggesting orthopyroxene.

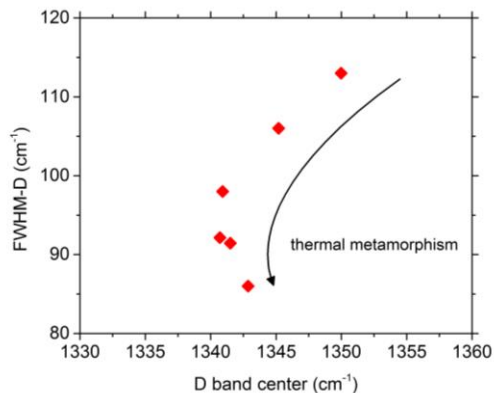


**Figure 3.** FWHM of D-band versus the D-band center frequency of multiple points extracted from the collected spectra. The curved arrow shows the direction of the thermal metamorphism trend.

The positions and FWHM of the D and G bands for several pixels are shown in Figures 3 and 4, respectively. The FWHM of the D band for the selected pixels span a wide range when compared to their peak positions, but mostly clustered near  $90\text{ cm}^{-1}$ . On the other hand, FWHM of the G band appears to be near  $70\text{ cm}^{-1}$  and higher for some pixels. The D-band parameters presented here are in agreement with that of CO chondrites reported by [6]. Based on the arrows in Figure 3 and 4, which show the direction of thermal metamorphism, there seem to be regions in the meteorite that have undergone different degrees of thermal alteration.

The distribution of organic matter in the Moss meteorite is reported to be highly heterogeneous [e.g., 5], and we see that different regions indicate different degree of disordered carbon. These suggest complex post-accretionary parent body alteration events. Organic matter in the Moss meteorite is reported [5] to indicate a higher thermal metamorphic grade than its assigned grade. Although we have only small number statistics, Figure 4 shows that Moss G band bandwidths are narrower (or more metamorphosed) than the CO3 data-point from [7], which is in agreement

with [5]. This indicates different thermal histories for Moss than for other members of the CO3 group. Furthermore, when compared to type 1 and 2 carbonaceous chondrites in Fig. 4, the peak position of the G band is consistent with a less disordered nature of the carbonaceous matter in Moss.

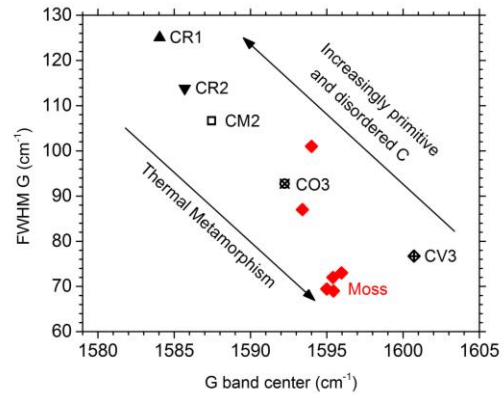


**Figure 4.** FWHM of G-band versus the G-band center frequency of multiple points extracted from the collected spectra, plotted with the other carbonaceous chondrites for comparison (data from [7], and references therein).

**Conclusions:** Micro-Raman spectra of the Moss CO3.6 meteorite show the presence of various silicate minerals as well as carbonaceous materials. Based on the D and G band parameters, carbon is more ordered than in other primitive carbonaceous chondrites, and points to a higher degree of metamorphism than other members of the CO group. Further micro-Raman imaging experiments will be conducted in order to increase the statistics for results of higher confidence. Additionally, micro-FTIR imaging experiments will be conducted for detection, identification, and distribution of chemical functional groups in order to better understand the mineralogy and organic content of the Moss meteorite, which will shed more light on parent body alteration histories.

**References:** [1] Connolly et al. (2007) MAPS, 42, 413–416. [2] Greenwood et al. (2007) LPSC XXXVIII, 2267. [3] Grady et al. (2002) MAPS, 37, 713–735. [4] Pearson et al. (2006) MAPS, 41 1891–1918. [5] Pearson et al. (2007) LPSC XXXVIII, 1846. [6] Busemann et al. 2011. CORALS II, 4086. [7] Jenniskens et al. (2012) Science, 338, 1583.

**Acknowledgements:** We would like to thank the American Museum of Natural History for providing the Moss meteorite for this study. This work is funded by the RIS<sup>4</sup>E node of NASA's Solar System Exploration Research Virtual Institute.